Effects of shikonin on the development of ovarian follicles and female germline stem cells

**Shu-Xin Ma[1,3,*], Li-Bo Tang[2,*] ⓘ,
Zhi-Hang Chen[1,3], Min-Li Wei[1], Zi-Juan Tang[1],
Yue-Hui Zheng[1], Guo Zong[4] and Jia Li[1] ⓘ**

Abstract
Objective: To investigate the effects and potential mechanism of action of shikonin (SHK) on the development of ovarian follicles and female germline stem cells (FGSCs).

Methods: Female Kunming adult mice were administered SHK (0, 20 and 50 mg/kg) by oral gavage. Cultures of FGSCs were treated with SHK 32 μmol/l for 24 h. The ovarian index in mouse ovaries was calculated. Numbers of primordial, primary and atretic follicles were counted. Germline stem cell markers and apoptosis were examined. Levels of glutathione (GSH), superoxide dismutase (SOD) and reactive oxygen species (ROS) were measured.

Results: Both doses of SHK significantly decreased the ovarian index, the numbers of primordial follicles, primary follicles and antral follicles in mice. SHK significantly increased the numbers of atretic follicles and atretic corpora lutea. SHK promoted apoptosis *in vivo* and *in vitro*. SHK significantly decreased the levels of the germline stem cell markers. SHK significantly lowered GSH levels and the activity of SOD in the peripheral blood from mice, whereas SHK significantly elevated cellular ROS content in FGSCs.

Conclusions: These current results suggested that follicular development and FGSCs were suppressed by SHK through the induction of apoptosis and oxidative stress might be involved in this pathological process.

[4]Shanghai Horizon Medical Technology Co., Ltd, Shanghai, China

*These authors contributed equally to this work.

Corresponding author:
Jia Li, Key Laboratory of Reproductive Physiology and Pathology of Jiangxi Province, District C, 999 Xueyu Avenue, Nanchang University, Honggutan New District, Nanchang 330006, Jiangxi Province, China.
Email: 492536343@qq.com

[1]Key Laboratory of Reproductive Physiology and Pathology of Jiangxi Province, Nanchang University, Nanchang, Jiangxi Province, China
[2]Second Clinical Medical College, Nanchang University, Nanchang, Jiangxi Province, China
[3]Queen Mary School, Jiangxi Medical College of Nanchang University, Nanchang, Jiangxi Province, China

Introduction

Shikonin (SHK) is a naphthoquinone compound extracted from the dried roots of Lithospermum erythrorhizon, a commonly used Chinese herbal medicine.[1] SHK and its derivatives have various pharmacological effects, such as immune surveillance,[2] oxidative equilibrium regulation[3,4] and anti-inflammatory actions.[5] Recently, SHK was shown to have robust anti-tumorigenic effects on colon cancer,[6] lung cancer[7] and other tumours *in vitro*.[8–10]

In contrast, several studies reported some deleterious effects of SHK on the reproductive system.[11–15] For example, in male mice, SHK damaged the spermatogenic epithelium, suppressed the process of spermatogenesis and impaired reproductive capacity through oestrogen receptor 1 (alpha) (*Esr1*) gene downregulation. In female mice, SHK inhibited the expression of oestrogen and attenuated its bioactivities through the regulation of oestrogen receptor α/NQO1 signaling.[11–13] In addition, SHK has pleiotropic effects on termination of pregnancy and infertility.[15] SHK caused the levels of various hormones to become ineffective, interfered with the growth of the uterus and ovulation, as well as disrupting the blood supply to the developing embryo.[15] Although SHK may be toxic to ovarian functions, a comprehensive investigation regarding the impact of SHK on follicular development is lacking. This current study was designed to investigate how SHK administration regulates the development of ovarian follicles.

Female germline stem cells (FGSCs) maintain the female reproductive functions and FGSCs have been extensively studied during the stages of oogenesis.[16] The ability to isolate FGSCs and study their proliferation enables the understanding of neo-oogenesis and ovarian recession.[17] This current study explored whether SHK controls the proliferation, differentiation and apoptosis of FGSCs. The imbalance between FGSCs and the stem-cell niche caused by oxidative stress contributes to ovarian recession.[18] In addition, oxidative stress impairs the stem-cell niche and induces follicular atresia.[16,17] The bioactivity of superoxide dismutase (SOD) and glutathione (GSH) counteracts the oxidative cytotoxicity induced by reactive oxygen species (ROS).[16–19]

To investigate the possible mechanism underlying the effects of SHK on ovarian follicular development and FGSCs, this current study measured the GSH concentration and the activity of SOD in the peripheral blood of mice. The levels of ROS in FGSCs treated with SHK were also measured.

Materials and methods

Animals

This study was conducted in the Key Laboratory of Reproductive Physiology and Pathology of Jiangxi Province, Nanchang University, Nanchang, Jiangxi Province, China and conformed to the National Research Council Guide for Care and Use of Laboratory Animals.[20] All animal

procedures followed the Institutional Animal Care and Use Committee rules and regulations.[20] All procedures involving mice were approved by the Animal and Ethical Committee of Nanchang University, Nanchang, Jiangxi Province, China.

Seven-week-old Kunming female mice were purchased from Jiangxi University of Traditional Chinese Medicine, Nanchang, Jiangxi Province, China and were housed under a 12-h light/12-h dark circle at 23°C with free access to food and water until they reached 2 months of age. Mice were randomly divided into three groups, five in each group. SHK (Meilunbio, Shanghai, China) powder was dissolved in a 10% sodium carboxymethylcellulose (CMC-Na) solution. The three groups were treated as follows: (i) the control group was administered 10% CMC-Na via oral gavage and the administered volume was lower than 2% of the total body weight; (ii) the low-dose group was administered 20 mg/kg SHK in CMC-Na via oral gavage; (iii) the high-dose group was administered 50 mg/kg SHK in CMC-Na via oral gavage. Two doses were given with an interval of 3 days between the two doses. Tissues and blood samples were collected 7 days after the last oral gavage.

Culture of FGSCs in vitro

The isolation, culture and proliferation of FGSCs were performed as described previously.[20,21] The ingredients of the tissue culture medium are listed in Table 1. Sandos inbred mice embryo-derived thioguanine-resistant, ouabain-resistant cells were used as the feeder cell line.

Ovarian weight and body weight

Ovaries were dissected under aseptic conditions and the ovaries were rinsed with 0.01 M phosphate-buffered saline (PBS, pH 7.4; Thermo Fisher, Shanghai, China). The organ coefficient was measured after complete drying of the ovaries as described previously.[22,23] Weight was measured using a precision electronic balance (Shimadzu, Fujian, Japan). The following formula was used to calculate the ovarian index: ovarian index (%) = ovarian weight (g)/mouse body weight (g) × 100.

Ovarian follicle quantification

Mice were sacrificed by cervical dislocation after blood collection. Ovaries were fixed in 4% paraformaldehyde overnight and embedded in paraffin.[24] Tissues were

Table 1. The ingredients used in the tissue culture medium for the culture of female germline stem cells.

Reagent	Supplier	Volume
Non-essential amino acids, 100×	Thermo Fisher Scientific, Rockford, IL, USA	100 μl
Fetal bovine serum	Invitrogen, Carlsbad, CA, USA	1 ml
Sodium pyruvate	Sangon, Shanghai, China	100 μl
L-glutamine	Ameresco, Framingham, MA, USA	100 μl
Leukaemia inhibitory factor	Sigma-Aldrich, St Louis, MO, USA	2 μl
Epidermal growth factor	Sigma-Aldrich, St Louis, MO, USA	1 μl
Basic fibroblast growth factor	Sigma-Aldrich, St Louis, MO, USA	1 μl
Glial cell-derived neurotrophic factor	Sigma-Aldrich, St Louis, MO, USA	1 μl
Mercaptoethanol	Sigma-Aldrich, St Louis, MO, USA	0.07 μl
Penicillin, 12 mg/ml	Sigma-Aldrich, St Louis, MO, USA	10 μl
Minimum essential medium-α	GIBCO® Cell Culture, Carlsbad, CA, USA	To bring the total volume up to 10 ml

sectioned into 5-µm sections and stained with haematoxylin and eosin. Images were obtained using an optical microscope (Olympus BX; Olympus, Tokyo, Japan). Quantification was performed as previously described.[25,26] The criteria for follicular classification for each structure was as follows: (i) primordial follicles were located in the superficial cortex, small in size and large in number. There was a layer of flat follicle cells around the oocyte; (ii) the primary follicle develops from the primordial follicle, which is larger than the primordial follicle and gradually penetrates into the deep cortex. The follicle cells surrounding the oocyte become multiple layers; (iii) the diameter of antral follicles was relatively large in clinical practice and the diameter can reach about 0.2 mm. Liquid is formed between granular cells to form a cavity; (iv) an atretic follicle is a type of degenerative follicles. The detachment of granulosa cells from the follicular basement membrane or the atrophy of granulosa cells will cause follicular atresia. After the follicle is atretic, fibrous connective tissue replaces the follicle; (v) atretic corpora lutea forms from atretic ovarian follicles and its granular cells undergo degeneration and destruction. The inner capsular cells undergo hypertrophy and change to form a luteal-like structure.

Immunohistochemistry and immunofluorescence

After dewaxing and rehydration, 5-µm thick paraffin sections were used for immunohistochemistry (IHC) and immunofluorescence (IF) according to a previous study.[27] For IF, paraffin sections were stained on a Dako Autostainer (Dako, Carpinteria, CA, USA) with a primary rabbit polyclonal antibody and an anti-rabbit secondary antibody (details below). For IHC, paraffin sections were stained on a Ventana Benchmark XT autostainer (Ventana Medical Systems, Tucson, AZ, USA). Antigen retrieval was performed with Ventana Cell Conditioner 1 (Ventana Medical Systems) for 30 min. Sections were then incubated with the primary rabbit polyclonal antibody at 37°C for 32 min. The primary antibodies used in this study were as follows: MVH (ab27591; Abcam, Shanghai, China) at a 1:100 dilution and OCT4 (11263-1-AP; Proteintech, Rosemont, IL, USA) at a 1:200 dilution. The proprietary Ventana anti-rabbit secondary antibody was then applied, followed by the diaminobenzidine solution (CAS91952; MERDK, Shanghai, China) used for the staining and chromogenic reactions. All of the images were examined under a NIKON Eclipse 80i microscope (Beijing Rongxing Guangheng Technology, Beijing, China).

TUNEL assay

The terminal deoxynucleotidyl transferase-mediated dUTP nick-end labelling (TUNEL) assay was performed using a TransDetect In Situ Fluorescein TUNEL Cell Apoptosis Detection Kit (TransGen Biotech, Beijing, China). 2-(4-amidino-phenyl)-6-indolecarbamidine dihydrochloride (DAPI) was used to counterstain the tissue sections and FGSCs. After washing three-times with 0.01 M PBS (pH 7.4), images were obtained using a fluorescence microscope (XSP-BM-13C; Olympus).

Quantitative polymerase chain reaction

Total RNA was extracted from ovaries using TRIzol® reagent (Thermo Fisher Scientific, Rockford, IL, USA) according to the manufacturer's instructions.[28] For the ovaries from the control group, 2–3 ovaries were required to extract sufficient total RNA. For the ovaries from the two experimental groups, 4–6 ovaries were required to extract enough RNA.

Approximately 2 µg RNA was used to synthesize cDNA using a PrimeScript® RT reagent Kit (TaKaRa Bio, Shiga, Japan). The amplification was performed on an ABI7000 PCR instrument (Applied Biosystems, Foster City, CA, USA). The cycling programme involved preliminary denaturation at 50°C for 2 min and at 95°C for 2 min, followed by 40 cycles of denaturation at 95°C for 15 s, annealing at 60°C for 60 s, followed by a final cooling step at 4°C.[29] The primers required for PCR are listed in Table 2. The reaction was carried out in a 20-µl volume containing 2 µl cDNA and other materials according to the manufacturer's instructions. β-actin was used as the internal reference gene. This process was repeated independently at least in triplicate to achieve good reproducibility. The relative levels of MVH and OCT4 mRNA were compared with those of β-actin and calculated using the $2^{-\Delta\Delta C_T}$ method. The C_T value used for these calculations was the mean of the triplicate for each reaction.

Cell proliferation assay

The viability of FGSCs *in vitro* was measured using the TransDetect Cell Counting Kit (CCK) (TransGen Biotech). A cell suspension was inoculated into a 96-well plate. After adding the 10% CCK solution, the cells were incubated in the dark for 4 h in a cell incubator (Sanyo, Hong Kong, China). The absorbance of the culture plate at 450 nm was measured using a BioTek microplate reader (Bio-Rad, Hercules, CA, USA).

Measurement of GSH and SOD

The concentration of GSH in the peripheral blood of mice was measured using a GSH enzyme-linked immunosorbent assay (ELISA) (Elabscience, WuHan, China). The activity of SOD was detected using a Total Superoxide Dismutase (SOD) Colorimetric Assay Kit (WST-1 method; Elabscience) according to the manufacturer's instructions. The minimum detectable concentrations were 0.94 µg/ml for GSH and 0.2 U/ml for SOD. Intra- and interassay coefficients of variation for all ELISAs were <6% and <5%, respectively.

ROS detection in cells

The levels of ROS were measured using a ROS Assay Kit according to the manufacturer's instructions (Nanjing Jiancheng Bioengineering Institute, Nanjing, China). 2,7-Dichlorodi-hydrofluorescein diacetate was added to the culture medium at 10 µM/l. The FGSCs were incubated at 37°C for 1 h and were then digested using trypsin. Cells were collected after centrifugation at 1000 *g* for 10 min at 4°C in a refrigerated high-speed centrifuge (Sorvall Stratos; Thermo Scientific, Shanghai, China). Fluorescence was detected using a fluorescence microscope (XSP-BM-13C; Olympus).

Table 2. The sequences of primers used for quantitative real-time polymerase chain reaction.

Gene	Forward primer (5′-3′)	Reverse primer (5′-3′)
β-actin	CATTGCTGACAGGATGCAGAAGG	TGCTGGAAGGTGGACAGTGAGG
Mouse vasa homolog	GTGTATTATTGTAGCACCAACTCG	CACCCTTGTACTATCTGTCGAACT
Octamer-blinding protein-4	AGCTGCTGAAGCAGAAGAGG	GGTTCTCATTGTTGTCGGCT

Statistical analyses

All statistical analyses were performed using GraphPad Prism 5 (Graphpad Software Inc., San Diego, CA, USA). All data were obtained from at least three separate experiments. Comparisons between experimental groups were analysed using unpaired Student's *t*-test. A *P*-value < 0.05 was considered statistically significant.

Results

After weighing each mouse and its ovaries in the control, 20 mg/kg and 50 mg/kg SHK treated groups, the ovarian indices of each group were calculated. The ovary-to-body weight ratio (ovarian index) is a straightforward method that is widely used to describe ovarian functions and the occurrence of ovarian atrophy.[23] SHK significantly decreased ovarian indices in both the 20 mg/kg ($P < 0.001$) and 50 mg/kg groups ($P < 0.001$), with significantly greater effects observed following 50 mg/kg administration compared with 20 mg/kg ($P < 0.001$) (Figure 1a). At the histological level, SHK disrupted ovarian structures (Figure 1b). To quantify the structural changes, the number of primordial follicles, primary follicles, antral follicles, atretic corpora lutea and atretic follicles were counted. SHK induced a reduction in the numbers of primordial follicles, primary follicles and antral follicles, with a more significant effect in the 50 mg/kg group ($P < 0.001$; Figure 1c). In contrast, the number of atretic follicles and atretic corpora lutea was increased significantly after SHK administration compared with the control
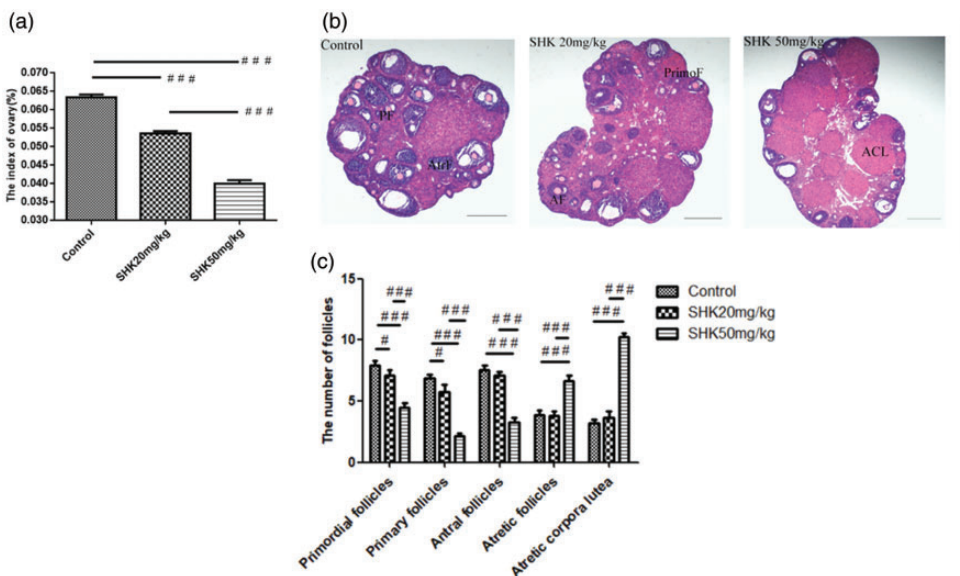

Figure 1. The effects of shikonin (SHK) on ovarian structure and phenotype ($n = 5$): (a) Ovarian indices of the control, 20 mg/kg and 50 mg/kg SHK treated groups. Data presented as mean ± SD. ###$P < 0.001$, unpaired Student's *t*-test; (b) The histological phenotype of control- and SHK-treated mouse ovary sections stained with haematoxylin and eosin. Scale bar 200 μm. PrimoF, primordial follicles; PF, primary follicles; AF, antral follicles; AtrF, atretic follicles; ACL, atretic corpora lutea; (c) The number of various ovarian follicles and atretic corpora lutea in the control, 20 mg/kg and 50 mg/kg SHK treated groups. Data presented as mean ± SD. #$P < 0.05$, ###$P < 0.001$, unpaired Student's *t*-test. The colour version of this figure is available at: http://imr.sagepub.com.
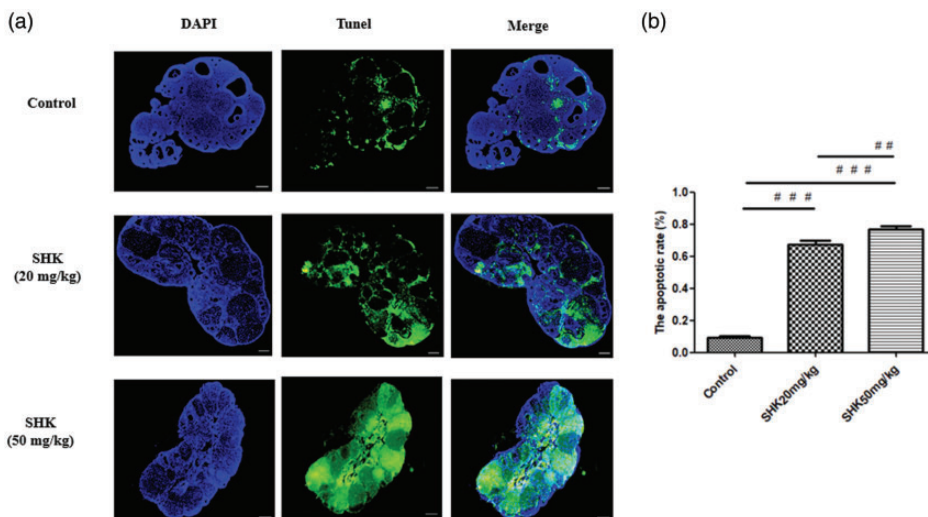
Figure 2. Terminal deoxynucleotidyl transferase-mediated dUTP nick-end labelling apoptosis assay of shikonin (SHK)-treated mouse ovaries. The cell nuclei are stained with 2-(4-amidinophenyl)-6-indolecarbamidine dihydrochloride (blue fluorescence) and the green fluorescent signals indicate apoptosis: (a) the intensity of apoptosis signals in the control, 20 mg/kg and 50 mg/kg SHK treated groups. Scale bar 100 μm; (b) The corresponding apoptotic rate in the control, 20 mg/kg and 50 mg/kg SHK treated groups. Data presented as mean ± SD. [##]$P < 0.01$, [###]$P < 0.001$, unpaired Student's t-test. The colour version of this figure is available at: http://imr.sagepub.com.

group ($P < 0.001$; Figure 1c). The differences in each of these five follicle types between the 20 mg/kg and 50 mg/kg SHK treated groups were significant ($P < 0.001$).

The levels of apoptosis in ovarian tissue sections were measured using TUNEL staining. The results showed that apoptosis occurred in the control group (Figure 2a). SHK administration significantly increased apoptosis at both concentrations compared with the control group ($P < 0.001$ for both comparisons; Figure 2b). The difference in the apoptotic rate between the 20 mg/kg and 50 mg/kg SHK treated groups was also significant ($P < 0.01$).

Previous studies have indicated that FGSCs are mainly located in the ovarian surface epithelium (OSE).[29,30] MVH is specifically expressed in all germ cell lineages and serves as a specific marker of reproductive cells.[31,32] OCT4 is specifically expressed in pluripotent stem cells.[33,34] As a result,

MVH and OCT4 were selected as the germline stem cell markers in the culture of FGSCs.[29] There was a concentration-dependent decrease in MVH and OCT4 mRNA levels as measured by PCR (Figure 3a). Significantly lower levels of MVH and OCT4 mRNA occurred in the 50 mg/kg SHK treated group compared with the control ($P < 0.001$) and 20 mg/kg SHK treated groups ($P < 0.001$). The mRNA transcription changes were confirmed using IHC (Figure 3b) and IF (Figure 3c), with 20 and 50 mg/kg SHK suppressing the levels of MVH and OCT4 in FGSCs.

The effects of SHK (0, 4, 8, 16, 32 and 64 μmol/l SHK) at 0, 24, 48 and 72 h on the viability of FGSCs was measured using a CCK kit. The 32 μmol/l dose for 24 h significantly affected cell viability compared with the control group ($P < 0.05$; Figure 4), so it was chosen for subsequent
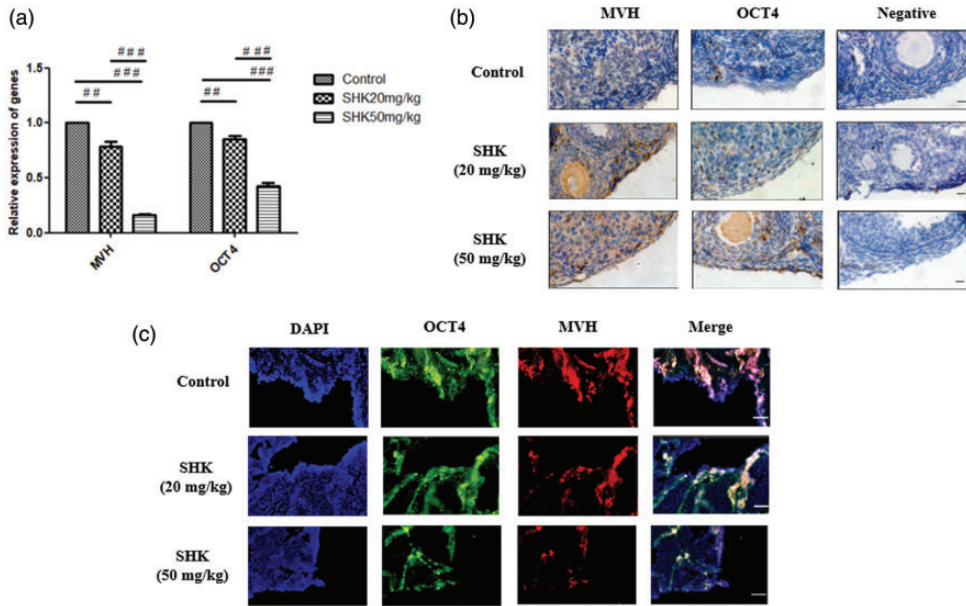
Figure 3. The levels of mouse vasa homolog (MVH) and octamer-blinding protein-4 (OCT4) in female germline stem cells: (a) quantitative real-time polymerase chain reaction analysis in the control, 20 mg/kg and 50 mg/kg shikonin (SHK) treated groups. Data presented as mean ± SD. $^{###}P < 0.01$; $^{####}P < 0.001$, unpaired Student's *t*-test; (b) immunohistochemical analysis in the control, 20 mg/kg and 50 mg/kg SHK treated groups. Scale bar 100 μm; (c) immunofluorescence analysis in the control, 20 mg/kg and 50 mg/kg SHK treated groups. Scale bar 20 μm. OCT is labelled green and MVH is labelled red. Staining of nuclei with 2-(4-amidinophenyl)-6-indolecarbamidine dihydrochloride (blue fluorescence) was also applied to each sample. The colour version of this figure is available at: http://imr.sagepub.com.
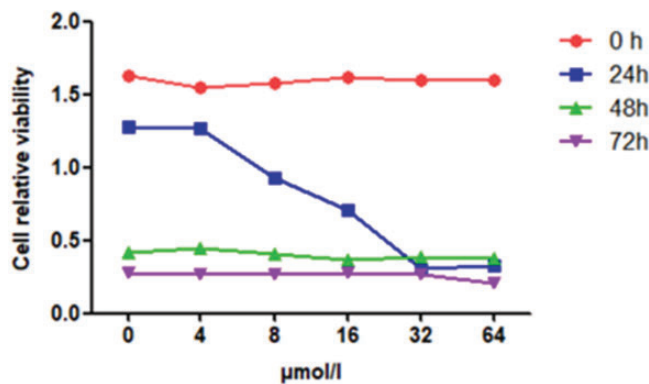

Figure 4. The effects of shikonin (SHK) treatment for 0–72 h at various concentrations on the viability of female germline stem cells *in vitro*. The 32 μmol/l SHK-treated group at 24 h demonstrated the most significant difference in cell viability compared with the control group ($P < 0.05$); unpaired Student's *t*-test. The colour version of this figure is available at: http://imr.sagepub.com.

experiments using FGSCs. Consistent with the *in vivo* results, TUNEL assays showed a significant increase in apoptotic cells after SHK treatment ($P < 0.001$; Figure 5).

Peripheral blood was collected from mice in order to measure the levels of GSH and SOD. The 50 mg/kg SHK treated group had significantly lower GSH content and suppressed SOD activity compared with the control and 20 mg/kg SHK treated groups ($P < 0.001$ for all comparisons; Figure 6).
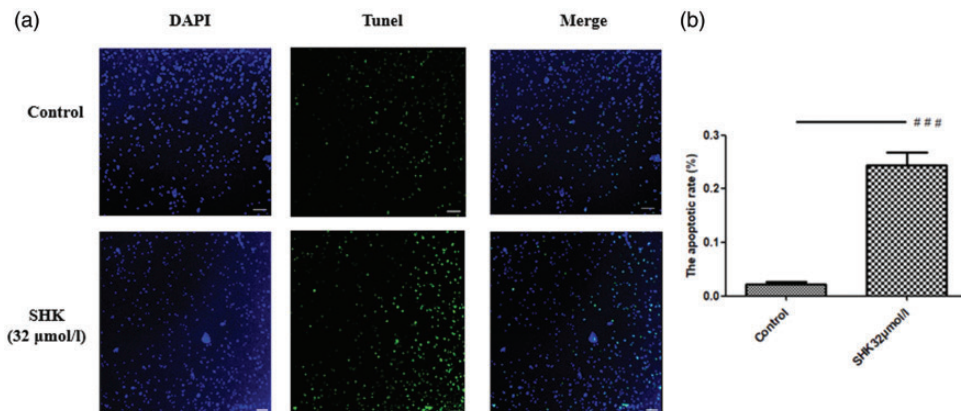

Figure 5. Terminal deoxynucleotidyl transferase-mediated dUTP nick-end labelling apoptosis assay of shikonin (SHK)-treated female germline stem cells *in vitro*. The cell nuclei are stained with 2-(4-amidino-phenyl)-6-indolecarbamidine dihydrochloride (blue fluorescence) and the green fluorescent signals indicate apoptosis: (a) the intensity of apoptosis signals in the control group and the 32 μmol/l SHK group treated for 24 h. Scale bar 50 μm; (b) The corresponding apoptotic rate in the control group and the 32 μmol/l SHK group treated for 24 h. Data presented as mean ± SD. ###$P < 0.001$, unpaired Student's *t*-test. The colour version of this figure is available at: http://imr.sagepub.com.
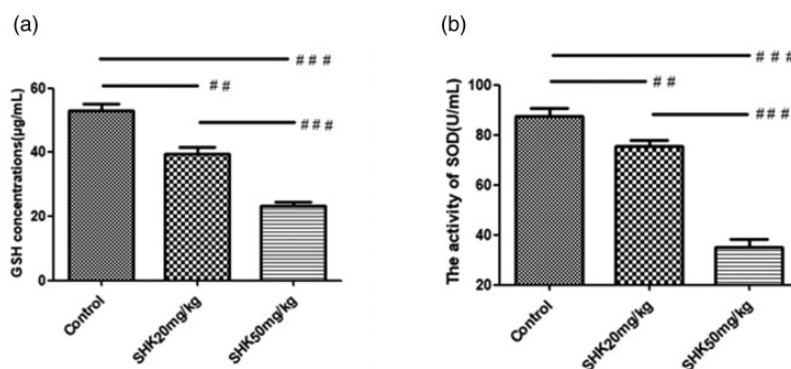

Figure 6. The changes in glutathione (GSH) and superoxide dismutase (SOD) levels in the peripheral blood of shikonin (SHK)-treated mice: (A) concentration of GSH in the control, 20 mg/kg and 50 mg/kg SHK treated groups. Data presented as mean ± SD. ##$P < 0.01$, ###$P < 0.001$, unpaired Student's *t*-test; (B) concentration of SOD in the control, 20 mg/kg and 50 mg/kg SHK treated groups. Data presented as mean ± SD. ##$P < 0.01$, ###$P < 0.001$, unpaired Student's *t*-test.

The accumulation of ROS is the leading cause of oxidate stress.[35] The ROS concentration in FGSCs were measured after SHK treatment at 32 µmol/l dose for 24 h and compared with ROS concentration at baseline in the control group (Figure 7). Treatment with SHK 32 µmol/l for 24 h caused a significant increase ROS levels in FGSCs compared with the control group ($P < 0.001$).

Discussion

Shikonin is a commonly used anti-tumorigenic medicine because of its apoptosis enhancing effects.[6] SHK is a novel immunosuppressant that is effective in a variety of diseases and clinical transplantation.[36,37] Previous reports using histological approaches demonstrated that SHK negatively regulated metabolic rates, hormone levels and reproductive functions.[11–15] However, the effects of SHK on ovarian follicular development and FGSCs and the underlying molecular mechanisms remain largely unclear.

The present study investigated the effects of SHK in oocyte development. These current results showed that SHK exhibited a dose-dependent effect on decreasing ovarian index, primordial follicles, primary follicles and antral follicles. SHK upregulated the numbers of atretic follicles and atretic corpora lutea. TUNEL methodology demonstrated that 50 mg/kg SHK significantly induced apoptosis, contributing to the blunted ovarian development and functional decline. In addition, SHK interrupts the endocrine system including the pituitary gland–ovary axis by interfering with the bioactivities of related hormones, such as follicle stimulating hormone, which subsequentially inhibits the maturation and ovulation of follicles in all grades.[14] This current study has identified a dose of SHK (50 mg/kg) that can effectively inhibit ovarian follicular development and reproductive functions in mice. This current study is the first comprehensive study on the biosafety of SHK during the development of ovarian follicles, providing an insight into drug safety in future female applications.
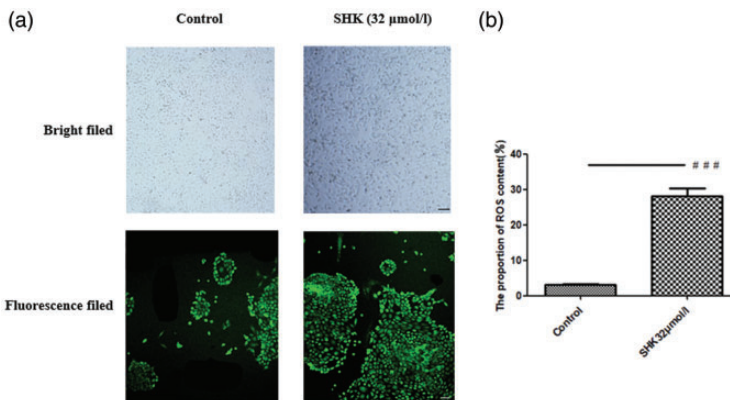

Figure 7. The concentration of reactive oxygen species (ROS) in shikonin (SHK)-treated female germline stem cells *in vitro*. The concentration of ROS is directly related to the intensity of the green fluorescent signals: (a) ROS in the control group and the 32 µmol/l SHK group treated for 24 h. Scale bar 50 µm; (b) The proportion of ROS in the control group and the 32 µmol/l SHK group treated for 24 h. Data presented as mean ± SD. ####$P < 0.001$, unpaired Student's *t*-test. The colour version of this figure is available at: http://imr.sagepub.com.

As a consequence of the apparent scarcity of FGSCs in ovaries,[38] it is difficult to access their response to drugs including SHK under regular laboratory conditions. In order to understand how SHK impacts on FGSCs and to provide future FGSC-related therapeutic approaches to restore ovarian function, this current study used the germline stem cell markers MVH and OCT4;[28,29] which were suppressed in the presence of SHK. The decline of MVH and OCT4 may suggest that FGSCs were disordered *in vivo*. Furthermore, SHK induced apoptosis in FGSCs *in vitro*. These adverse effects of SHK on FGSCs *in vivo* and *in vitro* may provide pharmacological antagonists to restore ovarian function in humans.

In order to study the mechanisms of SHK on ovaries and FGSCs, this current study measured the levels of molecules related to oxidative stress. The concentration of GSH and the activity of SOD were decreased by SHK in a dose-dependent manner *in vivo*. The content of ROS in FGSCs *in vitro* was significantly increased after SHK exposure. These important intracellular antioxidant molecules, GSH and SOD, are responsible for the elimination of ROS.[39,40] A previous study reported that SHK was able to control the expression of SOD and the content of GSH.[41] Consistent with this, these current results suggest that the reproductive-inhibitory effects induced by SHK might be brought about by interfering with the nonenzymatic or enzymatic antioxidant systems. SHK-induced increased oxidative stress might subsequentially damage the ovarian microenvironment in an irreversible manner, resulting in ovarian follicular death and atrophy, leading to the formation of degenerative corpora lutea. Future manipulation of these factors related to oxidative stress might increase the FGSC life span and reduce apoptosis.

In conclusion, this present study uncovered a novel mechanism by which SHK might induce infertility during SHK anti-tumorigenic application, which should be considered when using this drug in the clinic.

Declaration of conflicting interest

The authors declare that there are no conflicts of interest.

ORCID iDs

Li-Bo Tang https://orcid.org/0000-0002-4870-4408
Jia Li https://orcid.org/0000-0003-3226-4935

References

1. Boulos JC, Rahama M, Hegazy MF, et al. Shikonin derivatives for cancer prevention and therapy. *Cancer Lett* 2019; 459: 248–267.
2. Esmaeilzadeh E, Gardaneh M, Gharib E, et al. Shikonin protects dopaminergic cell line PC12 against 6-hydroxydopamine-mediated neurotoxicity via both glutathione-dependent and independent pathways and by inhibiting apoptosis. *Neurochem Res* 2013; 38: 1590–1604.
3. Chen CH, Chern CL, Lin CC, et al. Involvement of reactive oxygen species, but not mitochondrial permeability transition in the apoptotic induction of human SK-Hep-1 hepatoma cells by shikonin. *Planta Med* 2003; 69: 1119–1124.
4. Zhang N, Peng F, Wang Y, et al. Shikonin induces colorectal carcinoma cells apoptosis and autophagy by targeting galectin-1/JNK signaling axis. *Int J Biol Sci* 2020; 16: 147–161.

5. Guo C, He J, Song X, et al. Pharmacological properties and derivatives of shikonin – A review in recent years. *Pharmacol Res* 2019; 149: 104463.

6. He G, He G, Zhou R, et al. Enhancement of cisplatin-induced colon cancer cells apoptosis by shikonin, a natural inducer of ROS in vitro and in vivo. *Biochem Biophys Res Commun* 2016; 469: 1075–1082.

7. Hsieh YS, Liao CH, Chen WS, et al. Shikonin Inhibited Migration and Invasion of Human Lung Cancer Cells via Suppression of c-Met-Mediated Epithelial-to-Mesenchymal Transition. *J Cell Biochem* 2017; 118: 4639–4651.

8. Zhang S, Gao Q, Li W, et al. Shikonin inhibits cancer cell cycling by targeting Cdc25s. *BMC Cancer* 2019; 19: 20.

9. Yang YY, He HQ, Cui JH, et al. Shikonin Derivative DMAKO-05 Inhibits Akt Signal Activation and Melanoma Proliferation. *Chem Biol Drug Des* 2016; 87: 895–904.

10. Yang Q, Li S, Fu Z, et al. Shikonin promotes adriamycin induced apoptosis by upregulating caspase 3 and caspase 8 in osteosarcoma. *Mol Med Rep* 2017; 16: 1347–1352.

11. Yao Y, Brodie AM, Davidson NE, et al. Inhibition of estrogen signaling activates the NRF2 pathway in breast cancer. *Breast Cancer Res Treat* 2010; 124:585–591.

12. Hess RA, Zhou Q, Nie R, et al. Estrogens and epididymal function. *Reprod Fertil Dev* 2001; 13: 273–283.

13. Zhou Q, Clarke L, Nie R, et al. Estrogen action and male fertility: roles of the sodium/hydrogen exchanger-3 and fluid reabsorption in reproductive tract function. *Proc Natl Acad Sci U S A* 2001; 98: 14132–14137.

14. Findley WE and Jacobs BR. The antigonadotropic activity of Lithospermum ruderale I. The lack of steroid-like activity at the receptor level. *Contraception* 1980; 21: 199–205.

15. Yin ZF, Hu YZ and Su YH. Influence of Lithospermum on pregnancy. *Journal of Chinese Integrative Medicine* 2007; 5(5): 494–496 [Article in Chinese, English abstract].

16. Liu Y, Xu J, Zhu F, et al. Research advances in the regulation of the putative ovarian germline stem cell niche on female germline stem cells. *Syst Biol Reprod Med* 2019; 65: 121–128.

17. Zou K, Yuan Z, Yang Z, et al. Production of offspring from a germline stem cell line derived from neonatal ovaries. *Nat Cell Biol* 2009; 11: 631–636.

18. Banerjee S, Banerjee S, Saraswat G, et al. Female reproductive aging is master-planned at the level of ovary. *PLoS One* 2014; 9: e96210.

19. Carbone MC, Tatone C, Delle Monache S, et al. Antioxidant enzymatic defences in human follicular fluid: characterization and age-dependent changes. *Mol Hum Reprod* 2003; 9: 639–643.

20. Zhu X, Tian GG, Yu B, et al. Effects of bisphenol A on ovarian follicular development and female germline stem cells. *Arch Toxicol* 2018; 92: 1581–1591.

21. Wang H, Jiang M, Bi H, et al. Conversion of female germline stem cells from neonatal and prepubertal mice into pluripotent stem cells. *J Mol Cell Biol* 2014; 6: 164–171.

22. Zhao X, Liu Q, Sun H, et al. Chronic Systemic Toxicity Study of Copper Intrauterine Devices in Female Wistar Rats. *Med Sci Monit* 2017; 23: 3961–3970.

23. Zhu L, Li J, Xing N, et al. American ginseng regulates gene expression to protect against premature ovarian failure in rat. *Biomed Res Int* 2015; 2015: 767124.

24. Yang Y, Lin P, Chen F, et al. Luman recruiting factor regulates endoplasmic reticulum stress in mouse ovarian granulosa cell apoptosis. *Theriogenology* 2013; 79: 633–639.

25. Tilly JL. Ovarian follicle counts–not as simple as 1, 2, 3. *Reprod Biol Endocrinol* 2003; 1: 11.

26. Wang Y, Chang Q, Sun J, et al. Effects of HMG on revascularization and follicular survival in heterotopic autotransplants of mouse ovarian tissue. *Reprod Biomed Online* 2012; 24: 646–653.

27. Roden AC, Maleszewski JJ, Yi ES, et al. Reproducibility of Complement 4d deposition by immunofluorescence and

immunohistochemistry in lung allograft biopsies. *J Heart Lung Transplant* 2014; 33: 1223–1232.

28. Wang HF, Liu M, Li N, et al. Bisphenol A Impairs Mature Sperm Functions by a CatSper-Relevant Mechanism. *Toxicol Sci* 2016; 152: 145–154.

29. Pan Z, Sun M, Li J, et al. The Expression of Markers Related to Ovarian Germline Stem Cells in the Mouse Ovarian Surface Epithelium and the Correlation with Notch Signaling Pathway. *Cell Physiol Biochem* 2015; 37: 2311–2322.

30. Celik O, Celik E, Turkcuoglu I, et al. Germline cells in ovarian surface epithelium of mammalians: a promising notion. *Reprod Biol Endocrinol* 2012; 10: 112.

31. Encinas G, Zogbi C and Stumpp T. Detection of four germ cell markers in rats during testis morphogenesis: differences and similarities with mice. *Cells Tissues Organs* 2012; 195: 443–455.

32. Li R, Thorup J, Sun C, et al. Immunofluorescent analysis of testicular biopsies with germ cell and Sertoli cell markers shows significant MVH negative germ cell depletion with older age at orchiopexy. *J Urol* 2014; 191: 458–464.

33. Fan YX, Gu CH, Zhang YL, et al. Oct4 and Sox2 overexpression improves the proliferation and differentiation of bone mesenchymal stem cells in Xiaomeishan porcine. *Genet Mol Res* 2013; 12: 6067–6079.

34. Lawrence PA and Casal J. The mechanisms of planar cell polarity, growth and the Hippo pathway: some known unknowns. *Dev Biol* 2013; 377: 1–8.

35. Sieprath T, Corne TD, Willems PH, et al. Integrated High-Content Quantification of Intracellular ROS Levels and Mitochondrial Morphofunction. *Adv Anat Embryol Cell Biol* 2016; 219: 149–177.

36. Xu J, Jiang C, Wang X, et al. Upregulated PKM2 in Macrophages Exacerbates Experimental Arthritis via STAT1 Signaling. *J Immunol* 2020; 205: 181–192.

37. Zeng Q, Qiu F, Chen Y, et al. Shikonin Prolongs Allograft Survival via Induction of CD4+FoxP3+ Regulatory T Cells. *Front Immunol* 2019; 10: 652.

38. Pacchiarotti J, Maki C, Ramos T, et al. Differentiation potential of germ line stem cells derived from the postnatal mouse ovary. *Differentiation* 2010, 79: 159–170.

39. Wiegman CH, Michaeloudes C, Haji G, et al. Oxidative stress-induced mitochondrial dysfunction drives inflammation and airway smooth muscle remodeling in patients with chronic obstructive pulmonary disease. *J Allergy Clin Immunol* 2015; 136: 769–780.

40. Li L, Lai EY, Wellstein A, et al. Differential effects of superoxide and hydrogen peroxide on myogenic signaling, membrane potential, and contractions of mouse renal afferent arterioles. *Am J Physiol Renal Physiol* 2016; 310: F1197–F1205.

41. Guo H, Sun J, Li D, et al. Shikonin attenuates acetaminophen-induced acute liver injury via inhibition of oxidative stress and inflammation. *Biomed Pharmacother* 2019; 112: 108704.